Recent Results from the MRC/1Jy Survey

Source sizes, K-z relation and NICMOS imaging

Patrick J. McCarthy

Carnegie Observatory, 813 Santa Barbara St, Pasadena, CA 91101

1 Introduction

There are several basic issues that will occupy much of our discussion at this colloquium. They concern issues ranging from the micro-physics of scattering to the global evolution of galactic and radio source populations. There are essentially two approaches that our community applies to the study of radio galaxies: some dissect individual objects in great detail, while others use large samples to examine trends in global properties. Both are essential in building a well rounded picture of the workings of radio sources and their relationship to other classes of objects, be they AGNs or normal galaxies. One of the road blocks that we come up against time and again is the degeneracy between luminosity and look-back time in strong source samples such as the 3CRR. During the week we will hear from a number of groups that are addressing this issue through complete samples of sources with flux densities ranging from a factor of a few, to a few orders of magnitude, below the 10Jy limit of the 3CRR. These surveys are now being used to disentangle luminosity and evolutionary effects with some success.

It appears that we now have a reasonable rough sketch of the processes that shape the appearance of radio galaxies in the rest-frame visible and UV. The census of physical processes that are important is fairly complete, but we are now facing the realization that the mix of processes varies substantially from one object to another. The view that radio galaxies might form a fairly homogeneous population is becoming harder to support, even in the near-IR. We will see examples of objects that appear to be dominated by star formation (e.g. Dey et al. 1997) and equally compelling examples of objects dominated by scattering in the rest-frame UV (e.g. Cimatti et al. 1997) and even in the

λ4000 Å region of the spectrum.

One of the key issues that will be discussed here is the nature of the observed K-band emission and the meaning of the K$-z$ relation for strong sources. The suggestion by Eales & Rawlings (1996) that the K magnitude is correlated with radio power deserves careful examination, as its implications are far reaching. The current generation of near-IR arrays on 4 and 10-m telescopes is allowing the application of surface photometry to the problem of the evolution of the host galaxies (e.g. Rigler & Lilly 1994; Best et al. 1996; van Breugel et al. 1998). The recent advent of NICMOS offers us the means to observe the rest-frame visible continuum with the same spatial resolution now available in the spectacular WFPC2 images of the 3CRR and other samples.

In this contribution I shall discuss the status of the MRC/1Jy radio source sample and its application to the problems of the evolution of radio source sizes and the nature of the K$-z$ relation. I will show some early results from NICMOS imaging of radio galaxies with redshifts of ~ 2 and greater.

2 The MRC/1 Jy Radio Survey

Over the past several years Kapahi, van Breugel, Persson, Athreya and I have carried out a large survey of radio galaxies with flux densities near the peak of the 408 MHz source counts. The MRC/1Jy sample (McCarthy et al. 1996; Kapahi et al. 1997) is the largest sample of sources for which essentially complete optical and near-IR identifications are available. Its flux limit ($S_{408} > 0.95$Jy) is roughly a decade below the 3CRR (Laing et al. 1983) and while its redshift content ($\sim 75\%$) is less than optimal, it is nevertheless, well suited to a number of statistical investigations. In Figure 1 I show the run of P(408) vs. z for the MRC/1Jy and 3CRR samples. The strong, but spurious, correlation within each sample is the Malmquist bias, the gap between the two tracks results from the different solid angle coverages. The combination of the 3CRR and MRC/1Jy samples allows us to span a decade in power at any z and a wide range of z for a fixed radio power. The quasar sample has been compiled by Kapahi et al. (1997) and spectroscopy of nearly all of the QSR and BL Lac identifications was obtained by Hunstead et al. (1998). Baker & Hunstead (1996) have produced composite rest-frame UV spectra of the CSS, and core and lobe-dominated MRC/1Jy quasars.

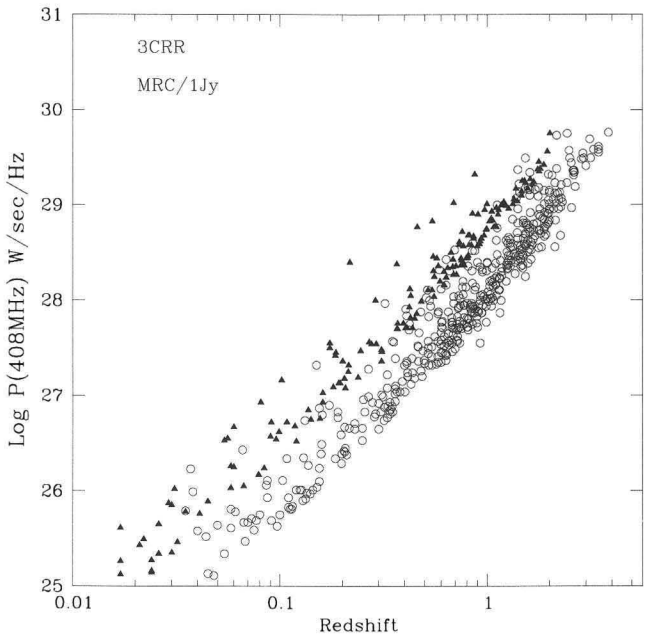

Figure 1. The run of 408MHz power with redshift for the 3CRR (filled symbols) and MRC/1Jy (open symbols) surveys.

3 Evolution of Radio Source Sizes

The MRC/1Jy sample is well suited to the study of source sizes. The sample is large and complete in the sense of containing $> 99\%$ of all sources above its flux limit. While the redshift content is not as complete as some other samples, the weak redshift dependence of the angular size allows the use of redshift estimates based on the apparent K magnitude. The determination of the power dependence is impacted more severely by the lack of complete spectroscopic redshifts, but the uniformity of the differences between our sample and the 3CRR from redshifts of order 0.5, where our redshift completeness is nearly 100%, to redshifts in the range from 1 to 2 suggests that our redshift estimates are robust.

There is a fair range of disagreement in the literature concerning the strength

of the evolution of source sizes and the nature of any dependence on radio power. Oort et al. (1987) and Kapahi (1989) used the 3CRR and LBDS samples to infer a strong evolution, going as $(1+z)^{-3.5}$ and a modest power dependence, $\sim P^{0.3}$. Neeser et al. (1995) used the highly complete 6C sample to infer a much weaker evolution and no power dependence.

What I present here is a fairly preliminary analysis of the sizes of the radio galaxies from the MRC/1Jy sample. Athreya (these proceedings) and Athreya et al. (1998) give a more complete treatment. In Figure 2 I plot the angular sizes of the 3CRR and MRC/1Jy radio galaxies. The large symbols are the medians in each of several redshift bins. The curves are the predicted median angular sizes for the two samples for the following redshift and power dependencies: $(1+z)^{-3.5}$, $P_{408}^{0.5}$, for a $q_0 = 0.1$ cosmology. The figure clearly shows that there is a systematic offset in the angular sizes between the two samples at any redshift, and hence a power dependence on the linear sizes. The parameterized curves do a fairly good job at reproducing the run of median sizes in the two samples. This analysis includes all of the sources not identified as quasars or BL Lacs and includes the CSS sources identified with galaxies.

The obvious question is why is this result so different from that obtained by Neeser et al. (1995). The flux limits of the 6C and MRC/1Jy samples are fairly similar for typical spectral indices. The main differences between the two samples are the selection frequency and the number of sources. The 6C with its 151MHz selection contains far fewer CCS sources than the MRC, and is in principle a better match to the 3CRR. Indeed Athreya et al. (1998) find a better agreement with Neeser et al. when excluding the CSS sources from the MRC sample. To some degree these results must be treated with care; it is not surprising that one finds a weaker evolution after removing all of the sources below 20 kpc. It is not clear that all of these are truly sources from a distinct population; some fraction of them may simply be smaller versions of the classical double sources. The order of magnitude difference in the size of the two samples renders the MRC much less susceptible to the impact of small number statistics.

4 Color and Luminosity Evolution of the Host Galaxies

The large formation redshift and passive evolution paradigm for radio galaxies is based largely on the uniformity of the K-z relation and the evolution of the red envelope in the visible and near-IR colors in the 3CRR and B2/1Jy samples

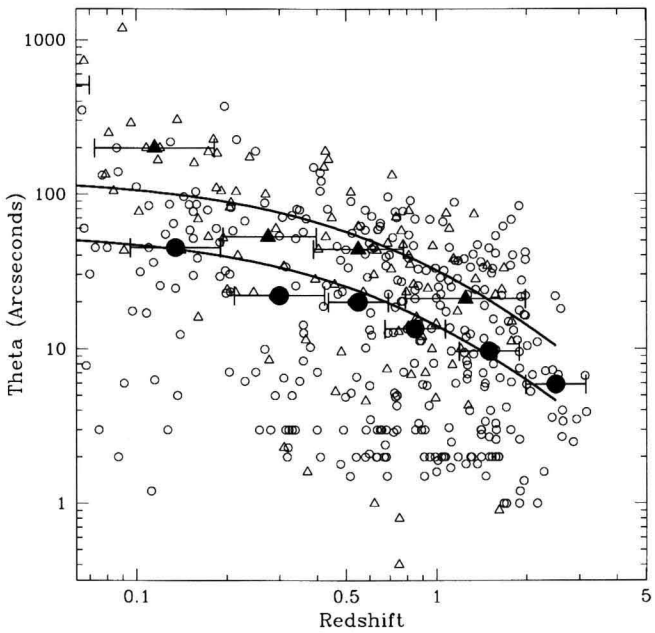

Figure 2. The angular sizes of galaxies from the 3CRR (triangles) and MRC/1Jy (circles) samples. The filled symbols are the medians in various redshift bins, the curves are the predicted angular sizes using the parameterization of the evolution and power dependencies given in the text.

(e.g. Lilly & Longair 1984; Eisenhardt & Lebofsky 1986; Lilly 1989). A similar behavior is seen in other samples (e.g. Dunlop et al. 1989). I illustrate this behavior for the MRC/1Jy sample in Figure 3 where I plot the $r-$K colors against z. The model curves show the colors of passively evolving systems with formation redshifts from 10 to 3 in a low Ω, H_0 Universe. For any redshift below ~ 2 there are galaxies with $r-$K colors are red as the passive evolution model and in J–K the galaxies continue to exhibit a similar behaviour out to $z \sim 2.5$.

In Figure 4 I plot the K-band Hubble diagram for the 3CRR, MRC/1Jy, and 6C samples along with an incomplete sample of high redshift radio galaxies from van Breugel et al. (1997). The data for the 6C sample were read from a plot in Rawlings (1997). I have removed a low order polynomial from the data

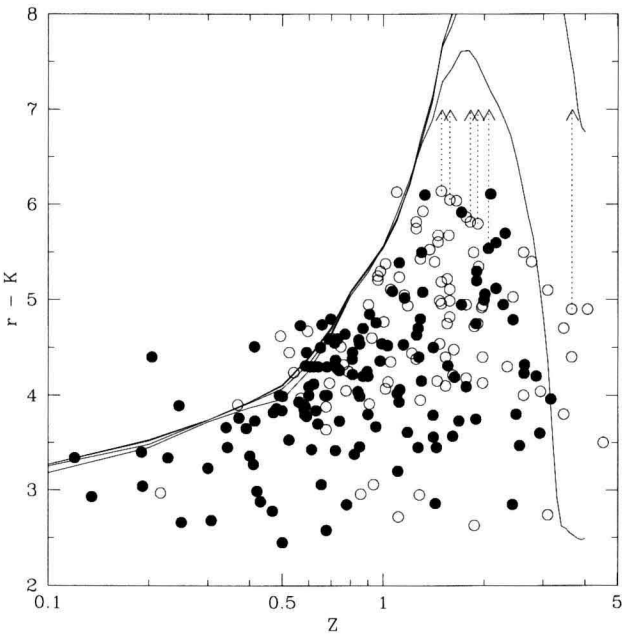

Figure 3. The r - K colors for galaxies in the MRC/1Jy sample. The filled symbols are objects with secure spectroscopic redshifts, the open symbols are objects for which the redshift has been estimated from the K magnitude. The solid lines are the same passive evolution model as above, but with formation redshifts ranging from 20 to 3.

to compress the vertical scale (this polynomial has no physical significance). The heavy open circles are the 3CRR, the light circles are the MRC/1Jy data, the triangles the 6C, and the squares are the van Breugel/NIRC sample. The filled circles and triangles are median values for the 3CRR and 6C samples, the diamonds are the MRC medians in various redshift bins, the error bars are $\pm 1\sigma$. The first point to note is the good agreement between the 3CRR and MRC/1Jy samples. The difference between the 3CRR and MRC samples is in the range $0 - 0.2$ magnitudes and is less than 1σ in each bin. The difference does appear to be systematic, with the MRC being fainter on average. The 6C sample shows the large, and increasing, departure from the 3CRR sample reported by Eales & Rawlings (1996). At $z > 1$ the 6C is 0.8 - 1.0 magnitudes fainter than the

3CRR. The apparent discrepancy between the 6C and MRC samples is puzzling, and I can see no obvious reason why it should occur. At redshifts of roughly 1.2 - 1.6 the MRC sample is significantly incomplete. Spectroscopic redshifts with CCDs is challenging in this redshift range, and it could well be that the faintest and reddest galaxies in this range have been preferentially lost from our sample of spectroscopic redshifts. At redshifts below one, I believe that the MRC is highly complete, and at $z \sim 0.5$, I am confident that we are nearly 100% complete. In this redshift range the MRC, 6C, and 3CRR are all consistent to within 1σ. The small offset between the 3CRR and MRC could easily arise from the differences in detectors and techniques used for each, compounded with the increased fraction of extended continuum in the 3CRR compared to weaker samples.

The solid line in Figure 4 is a minimal passive evolution Bruzual and Charlot (1993) model; the dotted line is the no-evolution K-correction. The 6C points follow the no-evolution line while the MRC and 3CRR samples are consistent with passive evolution and constant stellar mass.

5 Velocity fields in the extended emission-line regions

Baum, Spinrad and I have measured the extranuclear velocity fields in the emission-line gas for a large sample of radio galaxies. At redshifts below ~ 0.8 the typical radio galaxy has a velocity field with an amplitude of $100 - 300$ km s^{-1}. At larger redshifts the amplitudes increase to typically 800 km s^{-1}, with a number of systems having gas moving at more than 1000 km s^{-1}. Baum & McCarthy (1998) speculate that the apparently sudden change in velocity amplitudes reflects the change in galaxy environments. At these large redshifts radio galaxies are, on average, in richer environments than the low redshift FRII sources that comprise the bulk of the 3CRR and 1Jy sources with $0.2 < z < 0.5$. The merger picture for radio galaxies at these low redshift is quite consistent with the range of velocities seen in the ionized gas. The large amplitudes in the more distant systems are comparable to the velocity dispersions of rich clusters and suggest that galaxy collisions, rather than actual mergers, may be a more common form of dynamical interaction.

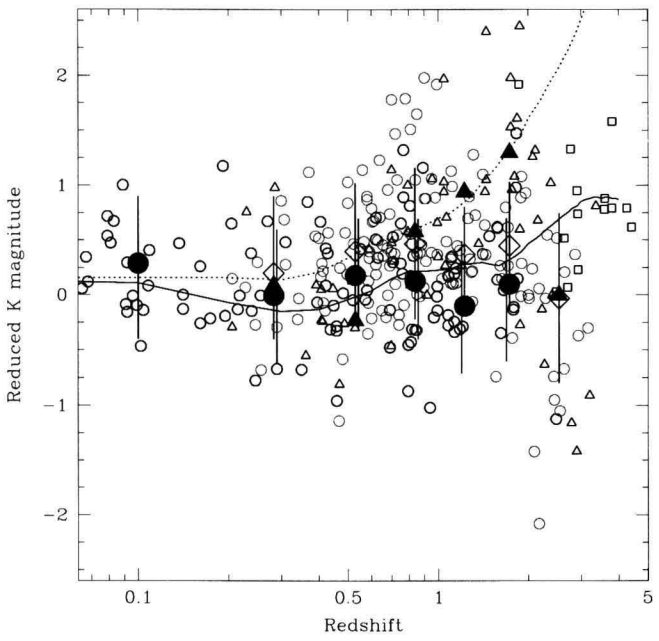

Figure 4. The K-band Hubble diagram for radio galaxies from the 3CRR, MRC/1-Jy surveys and a number of $z > 3$ radio galaxies taken from the literature. The dotted line is a no-evolution model with $H_0 = 50$ and $q_0 = 0.1$; the solid line is a BC96 passive evolution model with $z_f = 20$. A low order polynomial has been subtracted from both the data and the models to compress the scale. The heavy circles are the MRC, light circles 3CRR, triangles 6C and squares are the van Breugel et al. NIRC sample. The large symbols are the medians.

6 WFPC2 & NICMOS Imaging of Radio Galaxies with z > 2

Miley, Fosbury, van Breugel, Röttgering and I have imaged several $z > 2$ radio galaxies with NICMOS in the F160W bandpass. These observations benefit both from the large reduction in background compared to the ground and from diffraction limited images. In several cases we find that the H-band light is dominated by a nuclear point source. For several objects we find morphologies

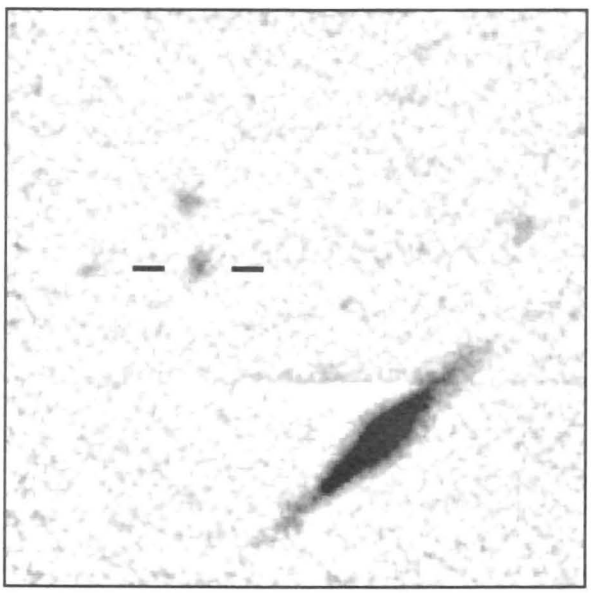

Figure 5. A NICMOS/F165M image of MRC 0324-228 ($z = 1.89$). The radio galaxy is marked with the two ticks. The close companion to the NE has colors similar to the radio source host. The image shown is $15'' \times 15''$.

that are consistent with normal early type galaxies. One of these is MRC 0324-228 ($z = 1.89$), shown in Figure 5.

In other cases we have detected resolved emission and have attempted to separate the contributions from a symmetric host galaxy and a component aligned with the radio axis. This separation is accomplished by using the WFPC2 and NICMOS images to iteratively solve for linear combinations of aligned and host galaxy contributions. In Figure 6 I show the WFPC2 and NICMOS images of MRC 0943-242 ($z = 2.93$). One can easily see that the F160W image contains a strong aligned component; the underlying symmetric component is less obvious. We find that the fractional contribution of the symmetric component, assumed to be stellar, is roughly 10% at F702W and 25% at F160W. In Figure 7 I show the spectral energy distribution of 0943-242 derived from ground-based imaging and from HST. The lower solid line is a Bruzual-Charlot model for a 1.5

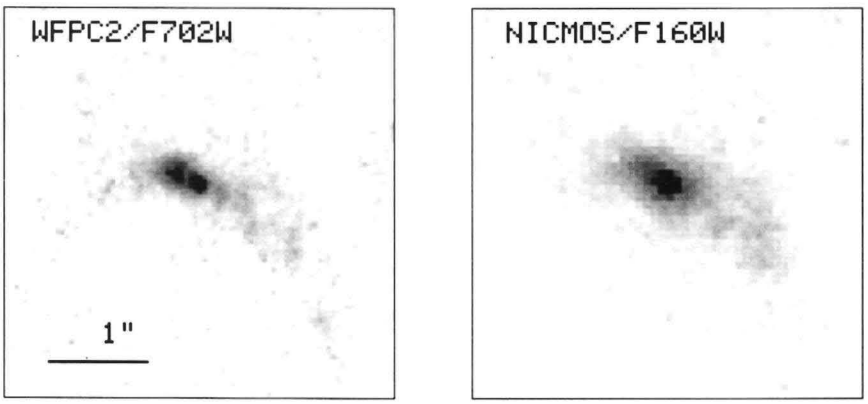

Figure 6. WFPC2/F702W and NICMOS/F160W images of the radio galaxy MRC 0943-242 ($z = 2.93$).

Gyr single-burst population and it is fitted to the photometry of the symmetric component. The dotted line is the observed composite SED for a core dominated MRC/1Jy quasar, as derived by Baker & Hunstead (1996). The upper solid line is the sum of the two components. The good agreement between the $4''$ aperture photometry and the model suggests that 0943-242 contains a large contribution from quasar continuum that is scattered by a nearly grey scattering medium. Extrapolating the model fit from the H-band to K-band yields a 30% contribution from the symmetric component.

In the case of 0943-242 we are confident that much of the observed H and K light is not associated with stars in a normal elliptical galaxy. The objects found to be dominated by nuclear point sources must also contain substantial non-stellar contributions. Thus the meaning of the colors and K magnitudes of the $z > 2$ galaxies with high radio powers is no longer clear. Our thinking regarding the evolution of the stellar populations in terms of an early formation redshift and subsequent passive evolution needs revision.

In Figure 8 I show an F160W image of MRC 0406-244 recently obtained with NICMOS. At $z = 2.43$ this image contains a contribution from nebular lines. The striking bipolar morphology revealed in this image is reminiscent of the wind-blown bubbles associated with Arp 220 and other ULIRGs. Deep WFPC2 imaging of this object by Rush et al. (1997) reveal an apparent double nucleus

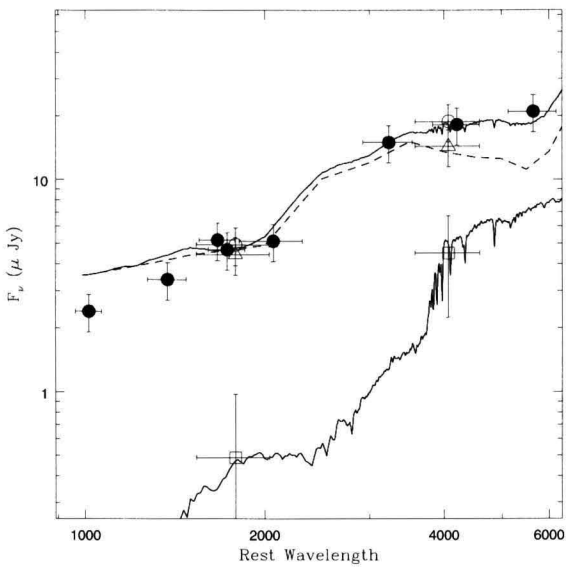

Figure 7. The derived SED for 0943-242. The open squares are the NICMOS and WFPC2 magnitudes for the host galaxy, the open triangles are the aligned component. The filled circles are the ground-based photometry. The model curves are described in the text.

and continuum features suggestive of tidal tails. It is tempting to speculate that this object may by a high redshift radio-loud analogue of the powerful ULIRGs and SNe driven outflows.

7 Summary

Our understanding of powerful radio sources and their relationship to other classes of AGN and star forming galaxies is undergoing considerable evolution at the present. The paradigms that work well for the local population of radio sources, and merger-driven activity in particular, may not be valid at early epochs. Imaging and spectroscopic observations show that the environments and dynamical states of radio galaxies evolve with look-back time. The application of NICMOS and ground-based near-IR imaging to the most distant radio galaxies

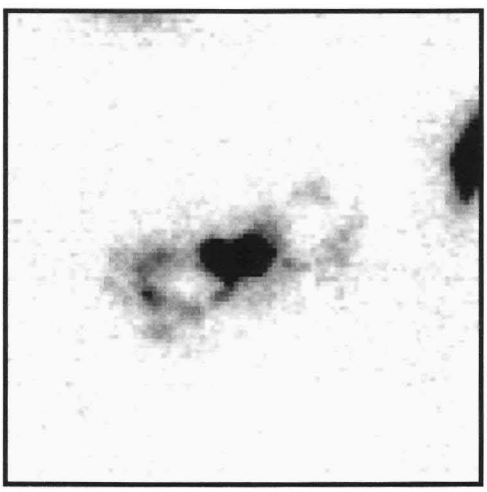

Figure 8. A NICMOS/F160W image of MRC 0406-244 ($z = 2.44$). The large bubble-like structures are aligned with the radio source axis and are likely to be composed of [OIII]5007,4959 and Hβ emission lines. The total size of the bipolar structure is 3.5″ or $\sim$ 30 kpc.

has led us to re-examine the basic assumptions that underlie our interpretation of the apparent color and luminosity evolution of these objects and their relation to early type galaxies.

Acknowledgements I thank my collaborators, as listed in the text, for allowing the use of previously unpublished data.

References

Athreya, R., McCarthy, P., Kapahi, V., van Breugel, W. 1998, A&A 329, 809
Baum, S. A., & McCarthy, P. 1998, ApJ, in prep
Baker, J., & Hunstead, R., 1996, 461, L59
Best, P., Longair, M., & Röttgering, H. 1996, MNRAS, 280, 9p
Bruzual, G. A., Charlot, S. 1993, ApJ, 405, 538

Cimatti, A., Dey, A., van Breugel, W., Hurt, T., Antonucci, R. 1997, 476, 677
Dey, A., van Breugel, W., Vacca, W., & Antonucci, R. 1997, ApJ, 490, 698
Dunlop, J. S., Guiderdoni, B., Rocca-Volmerange, B., Peacock, J. A., Longair, M. S. 1989, MNRAS, 240, 257
Eales, S. A., & Rawlings, S. 1996, ApJ, 460, 68
Eisenhardt, P. R. M. & Lebofsky, M. J. 1987, ApJ, 316, 70
Hunstead, R., Baker, J., Kapahi, V., Subramhanya, C. 1998, ApJS, in press
Kapahi, V. K. 1989, AJ, 97, 1
Kapahi, V. K., et al. 1997, ApJS, in press.
Laing, R., Riley, J., & Longair, M. 1983, MNRAS, 204, 151
Lilly, S. J., & Longair, M. S. 1984, MNRAS, 211, 833
Lilly, S. J. 1989 ApJ 340, 77
McCarthy, P., Baum, S. A., & Spinrad, H. 1996, ApJS, 106, 281
McCarthy, P., Kapahi, V. K., van Breugel, W., Persson, S. E., Athreya, R. M., & Subrahmanya, C. R. 1996, ApJS, 107, 19
Nesser, M. J., Eales, S. A., Law-Green, J. D., Leahy, J. P., & Rawlings, S. 1995, ApJ, 451, 76
Oort, M. J. A., Katgert, P., & Windhorst, R. 1987, Nature, 328, 500
Rawlings, S. 1997, preprint
Rigler, M. A., & Lilly S. J. 1994, ApJ, 427, 79
Rush, B., McCarthy, P., Athreya, R., & Persson, S. 1997, ApJ, 484, 163
van Breugel, W.J.M., Stanford, S.A., Spinrad, H., Stern, D., Graham, J.R. 1998, ApJ, 502, 614